Activation of Swell1 in microglia suppresses neuroinflammation and reduces brain damage in ischemic stroke

Baoyi Chen
Department of Neurosurgery, Shenzhen Key Laboratory of Neurosurgery, The First Affiliated Hospital of Shenzhen University, Shenzhen Second People's Hospital, Shenzhen 518035, China

Cong Xie
Department of Neurosurgery, The First Affiliated Hospital of Shenzhen University, Shenzhen Second People's Hospital, Graduate School of Guangzhou Medical University, Shenzhen 518035, China

Tengrui Shi
Department of Neurosurgery, Shenzhen Key Laboratory of Neurosurgery, The First Affiliated Hospital of Shenzhen University, Shenzhen Second People's Hospital, Shenzhen 518035, China

Shiqin Yue
School of Pharmaceutical Sciences, Health Science Center, Shenzhen University, Shenzhen 518035, China

Weiping Li
Department of Neurosurgery, Shenzhen Key Laboratory of Neurosurgery, The First Affiliated Hospital of Shenzhen University, Shenzhen Second People's Hospital, Shenzhen 518035, China

Guodong Huang
Department of Neurosurgery, Shenzhen Key Laboratory of Neurosurgery, The First Affiliated Hospital of Shenzhen University, Shenzhen Second People's Hospital, Shenzhen 518035, China

Yuan Zhang
Department of Neurosurgery, Shenzhen Key Laboratory of Neurosurgery, The First Affiliated Hospital of Shenzhen University, Shenzhen Second People's Hospital, Shenzhen 518035, China

Wenlan Liu (wlliu@szu.edu.cn)
Department of Neurosurgery, Shenzhen Key Laboratory of Neurosurgery, The First Affiliated Hospital of Shenzhen University, Shenzhen Second People's Hospital, Shenzhen 518035, China

---

Research Article

Keywords: Inflammation, Swell1, Chloride channel, Ischemia, Stroke, Microglial

Posted Date: March 21st, 2022

DOI: https://doi.org/10.21203/rs.3.rs-1436090/v1

Abstract

Background

Neuroinflammation and immune responses mediated by microglia are associated with brain injury after ischemic stroke, and it is novel that Cl^- movement and Cl-sensitive signal pathways have been shown to be implicated in the survival and switch of inflammation patterns of immune cells. Swell1, one of the components of Volume-regulated Cl^- currents (VRAC) is considered to be the main channels mediating Cl^- efflux from nerves cells. However, the role of Swell11 in ischemia-induced inflammation and the effect of Swell1 on the inflammation patterns switch of microglia remain unknown.

Methods

Whole-cell patch clamp recordings was used to examine Swell1-mediated VRAC in BV2 cells. In vivo and vitro studies comparing EGFP and Swell1 conditional knock-in mice were performed to determine the role of microglia Swell1 on inflammation and brain injury after ischemic stroke. In vitro experiments to further explored the mechanism of microglia Swell1 in regulating neuroinflammation.

Results

Our data showed that knockdown or overexpression of Swell1 in cultured BV2 cells inhibited or increased hypotonic-activated Cl^- currents, respectively, and these changes were completely blocked by the VRAC inhibitor DCPIB. Swell1 conditional knock-in mice promoted microglial survival in the lesion region, leading to reductions in neural cell apoptosis, infarction size and neurological deficits following transient middle cerebral artery occlusion (tMCAO). Using gene manipulating technique and pharmacological inhibitors, we further revealed that Swell1 opening led to SGK1 (a Cl^--sensitive kinase)-mediated activation of FOXO3a/CREB as well as WNK1 (another Cl^--sensitive kinase)-mediated SPAK/OSR1-CCCs activation, which promoted microglial survival and M2 polarization, thereby attenuating inflammation and ischemic brain injury.

Conclusion

Our results demonstrated that Swell1 is an essential component of microglia VRAC and its activation protects against ischemic brain injury through promoting microglial survival and M2 polarization, which provides new a new orientation for the treatment of ischemic stroke and other neurological diseases associated with inflammation.

Introduction

Ischemic stroke induces inflammation, oxidative stress, calcium overload and mitochondrial dysfunction in the ischemic brain region, among which the inflammation starts rapidly and lasts for a long time period ranging from several days to even months that provides a great possibility for post-stroke intervention and treatment[1,2]. The neuroinflammation and immune responses occurring minutes to hours after stroke were associated with the complex pathology of brain injury after ischemic stroke [3,4]. Many studies have shown that the CNS innate immune cells, i.e., the microglia, are the first inflammatory cells responding to ischemic insult and critically contribute to the prognosis of ischemic stroke through removing apoptotic cells and regulating inflammatory response in ischemic brain region[5,6]. However, whether microglia activation is detrimental or beneficial in ischemic stroke is largely dependent on their pro- or anti-inflammatory phenotype at specific pathophysiological stages and in specific brain regions after stroke, and this remains an unanswered important question in ischemic stroke[7,8].

Cerebral ischemia induces rapid activation and migration of microglia to the lesion sites, removing apoptotic cells and acting as an anti-inflammatory responder[9,10]. However, in most cases, there are not enough activated microglia that can timely remove all apoptotic cells, which leads to the necrosis of non-phagocytized apoptotic cells and the disruption of the phagocytic homeostasis in the ischemic brain region[11,12]. Non-phagocytized apoptotic cells may lead to an increase in the toxic intracellular response and induce the microglia switching from the anti-inflammatory (beneficial) phenotype (M2 type) to the pro-inflammatory (detrimental) phenotype (M1 type)[11,13]. Therefore, promoting the survival of microglia after ischemia and inducing their switch from the pro-inflammatory type to the anti-inflammatory type could reduce neuroinflammation and attenuate ischemic brain injury.

Excessive Na^+, Ca^{2+} influx and cell swelling in neurons and glial cells mediated by multiple transporters and channels are early phenomena of cerebral ischemia[14]. Cell swelling will initiate the regulation of volume reduction (RVD) process mediated mainly by volume-regulated anion channels (VRACs) that are widely expressed in astrocytes and neurons[15]. The VRACs share a homohexameric structure formed by the interaction of Swell1 (also known as LRRC8A) and four of its homologues (LRRC8B-E)[16–19]. Whole-cell patch clamp recording in brain slices has revealed that oxygen-glucose deprivation (OGD) significantly increases the amplitude of Swell1-dependent VRAC currents in hippocampal neurons and middle cerebral artery occlusion (MCAO) induces a transient increase in the protein level of Swell1 in the hippocampal tissue of mice[20]. Activation of Swell1 channel has been shown to mediate the non-vesicular release of glutamate from astrocytes and neurons, leading to increased brain damage after ischemic stroke[20,21]. Meanwhile, Swell1 appears to be essential for mice survival, as deletion of Swell1 in hippocampal neurons leads to their death[20,22,23]. We have previously demonstrated that the opening of VRACs activates Cl^--sensitive kinases WNK1 and SGK1, which promotes the survival of cerebrovascular smooth muscle cells[24,25]. In addition, Swell1-mediated Cl^- movement may contribute to the regulation of inflammatory patterns in phagocytes, as defects in the Cl^- flux and Cl^- sensing pathway WNK1–SPAK/OSR1–CCCs (Cation-Chloride Cotransporters) promote the switch of phagocytes to the pro-

inflammatory type[26]. However, the presence of Swell1 in microglia and its function in ischemic brain injury, remains unclear.

In the present study, we applied electrophysiological, genetic and pharmacological approaches and studied the role of microglial Swell1 in ischemic stroke. Our data demonstrated that Swell1 was essential for swelling-activated Cl^- current and VRACs in microglia. Moreover, Swell1-mediated Cl^- efflux could activate Cl^--sensitive kinase WNK1 and SGK1, which in turn promoted the survival and M2-polarization of microglia through FOXO3a/CREB and SPAK/OSR1-CCCs signaling pathways and led to a reduction in neuroinflammation and ischemic brain damage. These results may provide a basis for targeting VRACs for the treatment of ischemic stroke as well as other inflammatory neurological diseases.

Material And Methods

1. Reagents and antibodies

Cell culture medium (DMEM), fetal calf serum, bovine serum albumin (BSA), and cocktail were obtained from GIBCO/Invitrogen. Lipofectamine 2000, Combined Protease and Phosphatase Inhibitors were from ThermoFisher Scientific Inc. Anti-Swell1, anti-FOXO3a, anti-phospho-FOXO3a (Ser316), anti-CREB and anti-Phospho-CREB (Ser133) were from Cell Signaling Technology. TUNEL Assay Kit, anti-TMEM119, anti-WNK1, anti-Phospho-WNK1 (Thr58), FITC-conjugated secondary antibodies, Cy5-conjugated secondary antibodies and DAPI Staining Solution were from Abcam. Anti-NeuN, anti-SGK1 and anti-phospho-SGK1 (Ser422) were purchased from Merck Millipore. Anti-SPAK, anti-OSR1 and anti-NKCC1 were from ThermoFisher. Anti-phospho-SPAK (Ser380), anti-phospho-OSR1(Ser315) and anti-phospho-NKCC1(Thr203) were from CUSABIO. Hyperfect Transfection Reagent (HiPerfect) was purchased from QIAGEN. Cell Counting Assay Kit-8 was purchased from Dojindo Molecular Technologies. Annexin V-PE/7-AAD Apoptosis Detection Kit and Cell Cycle Analysis Kit (PI) were purchased from Keygen Biotech. DCPIB was purchased from Tocris Bioscience, GSK65394 and WNK463 were purchased from MedChemExpress. Other chemicals, if not indicated, were all purchased from Sigma-Aldrich.

2. Animals and treatment

Male transgenic mice (C57BL/ Cx3cr1- Cre) weighing 18-20 g (3-4 weeks old) were purchased from Cyagen (Suzhou) Biotechnology. Mice were injected pAAV-CMV-DIO-EGFP-tWPA (100 μl, $1*10^{12}$ v.g./ml) or pAAV-CMV-DIO- LRRC8A-3×FLAG-tWPA (100 μl, $1*10^{12}$ v.g./ml) virus designed by OBiO Technology (Shanghai), through tail vein and housed in a temperature-controlled environment with a 12 h-light-dark cycle and allowed free access to food and water for 21 days. Prior to experiments, the mice were randomized into indicated experimental groups and the indices were measured by the researcher blinded to treatment.

3. In vivo focal ischemic stroke model

The mice were subjected to 1 h of middle cerebral artery occlusion (MCAO) with 24 h of reperfusion. In brief, the mice were subjected to 3% isoflurane for an anesthesia induction, thereafter with 1-1.5% isoflurane maintenance during the whole procedure. During the operation, rectal temperature was maintained at 37.0±0.5 °C by a heating pad (ALC-HTP homeothermic system, Alcott Biotech, Shanghai, China). Focal cerebral ischemia was induced by inserting a 0622-0624 monofilament (YUSHUN, Guangzhou, China) into the left internal carotid artery via the common carotid artery. After 1 h of occlusion, the filament was removed and the skin incision was sutured. Mice were returned to their cages and were sacrificed 24 h after reperfusion. All animals had free access to food and water following the procedure.

4. Evaluation of neurological score

Neurological score was assessed an investigator blinded to animal grouping at 24 h after cerebral ischemia according to a protocol (Longa Scoring Method) described [27]. The scoring was based on the following tests: 0 point, the mice moved normally; 1 point, the mice could not fully stretch their left front legs; 2 points, the mice turned around in a circle; 3 points, the mice fell on their left side; 4 points, the mice could not move by themselves and lost consciousness.

5. Rotarod test

Animals were placed on an accelerating rotating rod (from 4 to 40 rpm over 300 s) and their latency to fall was recorded. Preoperative training was performed for 3 days with 3 daily trials (total 15min), and most of the mice could maintain on the rod for 260-300s, with the last time trial serving as a preoperative baseline. The pre-trained animals (n = 9) were subjected to tMCAO as described above, and then the animals were placed on the rotating bar to evaluate the time of permanence.

6. 2, 3, 5-Triphenyltetrazolium chloride (TTC) staining

After neurological evaluation, brains were removed and cut into five 1-mm serial coronal sections. The sections were stained with 1.5% TTC (T8877, Sigma, St. Louis, MO, USA) in PBS for 5 min at 37°C. The TTC stained sections were photographed and digitized. Using Image-Pro Plus, the areas of TTC negative and the ipsilateral hemisphere were measured. The volume of infarct was calculated and expressed as the sum area of infarct/the sum area of brain slice.

7. Cell culture and transfection

BV2 cells were purchased from ATCC. The cells were maintained in DMEM supplemented with 10% fetal bovine serum (FBS) and 1% penicillin/ streptomycin (P/S) at 37℃ in a humidified incubator gassed with 95% CO_2. Swell1 overexpressing adenovirus that expressed mouse Swell1 (NM_177725.4) with an EGFP (green fluorescent protein) tag and its negative control were purchased from OBiO Technology. BV2 were transfected with the adenovirus according to a previously described method[24]. Swell1 small interfering RNA (siRNA) (5'GCCUGCAUUGGUUUGCCAATT3') and Scrambled RNA (5'UUCUCCGAACGUGUCACGU-3')

were designed and synthesized by Qiagen. Scrambled RNA was used as a negative control. Plasmids with RFP tag were designed and produced according to these small interfering RNA chain sequence and used for cell labeling in patch clamp experiments. Swell1 siRNA and negative control siRNA (or Plasmids) were transfected into BV2 by using HiPerfect (or Lipofectamine 2000) transfection reagent according to a previously described protocol[24].

8. Microglia electrophysiology

BV2 cells were seeded on glass coverslips (diameter 12 mm) and cultured for at least 24 h in DMEM until fully adherent. For hypotonicity-activated VRAC current recordings, BV2 cells were whole-cell patched in isotonic bath solution containing 90 mM NMDG-Cl, 2 mM KCl, 1 mM MgCl2, 2 mM CaCl2, 10 mM HEPES, 10 mM glucose, 100 mM mannitol (305 mOsm/kg, pH 7.3 adjusted with NMDG) or in a hypotonic solution that had the same ionic composition as isotonic bath solution except no mannitol (212 mOsm/kg, pH 7.3 adjusted with NMDG). Recording electrodes (3-5 MΩ) were filled with a standard internal solution containing 133 mM CsCl, 10 mM HEPES, 4 mM Mg-ATP, 0.5 mM Na3-GTP,2 mM CaCl2, 5 mM EGTA (pH 7.2 adjusted with CsOH and osmolality was 295-305 mOsm/kg). For the step protocol, cells were held at -60 mV and voltage step pulses (5 s interval, 500 ms duration) were applied from -100 to +100 mV in 20 mV increments. For the VRAC time course, constant voltage ramps (5 s interval, 500 ms duration) were applied from a holding potential of 0 to 100 mV.

9. Oxygen and glucose deprivation (OGD) and reoxygenation treatment

OGD was used to mimic ischemic conditions for microglia in vitro as described previously[28]. Briefly, BV2 cells were transfected and cultured for 24 h in DMEM, and were then incubated in a self-contained and sealed hypoxia incubator chamber (Billups-Rothenberg) (5% CO2 and 95%N2) for 1 h in DMEM without serum and glucose. After 1 h of exposure to OGD challenge, the cultures were removed from the anaerobic chamber, and the OGD medium was replaced with normal culture medium. The cells were then allowed to recover for 24 h before examinations of cell viability, flow cytometry or q-PCR.

10. Immunostaining

For animal studies, anesthetized mice were perfused transcardially with PBS, followed by 4% PFA in PBS. Brains were removed and post-fixed in 4% PFA at 4°C overnight. After dehydration by 30% sucrose, brains were embedded in OCT (Tissue-Tek) and cut into 10 μm-thick sections on cryostat microtome (Leica). For cellular studies, the BV2 cells were post-fixed in 4% PFA at room temperature (RT) for 15 minutes after washing with PBS. The brain sections and BV2 cells were permeabilized with 0.2% Triton X-100 and 1% BSA in PBS for 45 min at room temperature (RT), washed three times with PBS, blocked in 10% BSA, and incubated with anti-Swell1, anti-TMEM119 or anti-NeuN (1:200) at 4°C overnight. After washing three times with PBS, the samples were incubated with Fluor-conjugated secondary antibody (1:500) for 1 h at RT, followed by DAPI staining. Images were taken under Zeiss LSM780 confocal microscope.

11. Western blot

Cultured BV2 cells were lysed in RIPA with 1% protease inhibitors cocktails and 1% phosphatase inhibitor cocktails. After centrifugation at 15,000 g for 15 min at 4 ◦C, the supernatant was obtained, and the protein concentration was measured with a BCA Kit (Beyotime). Fifty μg proteins from each sample were subjected to polyacrylamide gel electrophoresis and transferred to a polyvinylidene difluoride membrane. The membrane was blocked with 5% milk (or 5% BSA for protein phosphorylation assay) in Tris-buffered saline buffer at RT for 1 h, and then add primary antibody (1:500 or 1:1000) and incubate overnight at 4°C. After wash with TBS buffer for 3 times, the membranes were incubated with HRP-conjugated secondary antibody (1:2000, Cell Signaling Technology) in the same TBS buffer for 1 h at RT. The blots were detected by a scanner (Bio-Rad) and analyzed with ImageJ (NIH).

12. Cytokine detection

Cytokine levels in mice serum and tissues of mice brain were measured using a multiplex cytokine/chemokine assay (Bio-Plex 23-plex Mouse cytokine assay; Bio-Rad), according to the manufacturer's instructions. The concentrations of IL-1β, IL-6, IL-10, and TNF-α in BV2 cell lysates were measured by enzyme-linked immunosorbent assay (ELISA). Quantification of these cytokines was performed with the corresponding kits according to the manufacturer's protocol.

13. CCK-8 assay for cell viability

Cell viability was measured by the CCK-8 method according to a previously described protocol[24]. In brief, BV2 cells were seeded into 96-well plates and tested 24 h after transfection and OGD treatment. Cells growth was arrested by incubation in DMEM with 0.5% fetal bovine serum for 24 h before the OGD treatment. Then, 10 μl of CCK-8 solution was added to each well and incubated for another 2 h before measuring the absorbance at 450 nm with a microplate reader (Bio-Tek).

14. Quantification of apoptosis and cell cycle transition by Flow cytometry

BV2 cells were cultured in 6-well plates at 70% confluence and were transfected with Ad-Swell1 or Swell1 siRNA for 24 h before exposing to 1 h OGD and 24 h reoxygenation. For apoptosis assessment, the cells were harvested for Annexin V-PE and 7-AAD staining using the Annexin V-PE/7-AAD Apoptosis Detection Kit according to manufacturer's instructions. The stained cells were counted by flow cytometry analysis (Coulter, Hialeah, FL). For data analysis, the cells in the lower right, upper right, lower left and upper left corners represented the early apoptotic cells, late apoptotic cells, the survival and necrotic cells, respectively. For cell cycle analysis, the cells were fixed in ice-cold 70% ethanol/PBS, and then treated with ribonuclease A (0.2 mg/mL) before staining with propidium iodide at 4°C overnight. Minimums of 10,000 events were recorded for each sample. The data were tabulated as the sum of cells in S, G0/G1 and G2 phase and normalized as a fold change of the normal controls.

15. Real-Time PCR

Total RNA was extracted from cultured BV2 cells using TRIZOL reagent (Invitrogen) according to the manufacturer's guidelines. Then, cDNA was synthesized using PrimeScript RT reagent Kit (Takara), qPCR reactions were performed in triplicate with TB Green Premix Ex Taq II (Takara) on an Applied Biosystems 7500 Real-Time PCR Detection System (Applied Biosystems). Relative gene expression was normalized to the housekeeping gene GAPDH (or β-actin) and calculated using the $2^{-\Delta\Delta Ct}$ method. The primers used for amplification are shown in supplement: Table S1.

16. 4D label-free phosphorylation modification proteomics

The proteomics experiment was done by PTM BioLab (Hangzhou, China) using a standard protocol[29]. Briefly, the BV2 cells were removed from -80°C storage, and processed through the steps of protein extraction, trypsin digestion, affinity enrichment of the phosphopeptides, and then were detected by LC-MS/MS analysis. The resulting MS/MS data were processed using the MaxQuant search engine (v1.6.6.0). Protein annotation and functional enrichment were analyzed by Gene Ontology (GO) annotation and KEGG pathway annotation. For phosphoproteome, software MoMo (motif-x algorithm) was used to analyze the model of sequences constituted with amino acids in specific positions of modify-21-mers (10 amino acids upstream and downstream of the site, respectively) and modify-13-mers for phosphorylation (6 amino acids upstream and downstream of the site) in all protein sequences.

17. Statistical Analysis.

Data analysis was performed using GraphPad Prism 9 (GraphPad software Inc). All data are represented as the mean ± S.E.M. Statistical significance was calculated by Tukey's multiple comparisons test, one- or two-way ANOVA followed by Bonferroni multiple comparisons test. n value represents the number of independent experiments. Statistical significance was set at *$p \leq 0.05$, and denote $p \leq 0.01$ or 0.001 as **p or ***p, respectively.

Results

Swell1 is essential for VRAC activity in microglia

Swell1 (LRRC8A) is a component of the swelling-activated Cl^- current ($I_{Cl,SWELL}$) channels or VRACs that are widely expressed in astrocytes and neurons[15]. To determine whether Swell1 is essential for the activity VRACs in microglia, we first exposed BV2 cells to a hypotonic solution to induce cell swelling and measured transmembrane currents using whole-cell patch clamp technique. As shown in Fig. 1A, the perfusion of hypotonic solution elicited a sharp increase in the transmembrane current, and this current was completely blocked by the specific Cl^- current channel inhibitor 4-(2-butyl-6,7-dichloro-2-cyclopentyl-indan-1-on-5-yl) oxobutyric acid (DCPIB). Of note, this DCPIB-sensitive Cl^- current showed mild outward rectification (Fig. 1A, 1B), which coincided well with the characteristics of VRAC and supported the existence of VRACs in microglia. To further demonstrate a role of Swell1 in microglial VRACs, we manipulated Swell1 expression in BV2 cells using siRNA plasmids or adenovirus vectors and

assessed their effects on VRACs. Swell1 siRNA plasmids (10, 20 or 40 nM) (Swell1 SI) substantially reduced Swell1 expression at 48 h after transfection (Fig. S1A), and Swell1 adenovirus (Ad-Swell1) significantly upregulated Swell1 expression after transfection with 50, 100 or 200 multiplicity of infection (MOI) for 48 h (Fig.S1B). Since 20 nM Si-Swell1 and 100 MOI Ad-Swell1 could effectively manipulate Swell1 expression, these doses were chosen for the rest of the experiments in this study. Using these two genetic tools, we found that hypotonicity-induced Cl^- currents in BV2 cells were significantly suppressed or augmented when Swell1 was knocked down or overexpressed, and the augmentation of hypotonicity-induced Cl^- current by Ad-Swell1 was completely inhibited by DCPIB (Fig. 1B, 1C and 1D). Lastly, to visualize the location of Swell1 in microglia, we performed immunofluorescence-staining experiments and showed that Swell1 was mainly distributed on the cell membrane and partly in the cytoplasm (Fig 1E). Taken together, these results indicated that Swell1 is essential for maintaining the normal function of VRACs in microglia and its upregulation significantly enhances Cl^- efflux in BV2 cells.

Swell1 overexpression in microglia provides neuroprotection against ischemic stroke

To determine whether Swell1-dependent VRACs in microglia play a role in ischemic brain damage, we generated microglial-specific Swell1 overexpression mice by transfecting Cx3cr1-Cre mice with pAAV-CMV-DIO-LRRC8A-3×FLAG-tWPA or control pAAV-CMV-DIO-EGFP-tWPA viral vectors. The specificity of Cre-dependent expression of Swell1 in Cx3cr1-Cre mice was confirmed by the co-localization of TMEM119-cy5 (red) and EGFP (green) or Swell1/FITC (green) (Fig. S2). Using these transgenic mice, we conducted tMCAO and assessed the effects of Swell1 overexpression on infarct size and, neurological deficits in Cre-EGFP and Cre-Swell1 mice. As shown in Fig 2A, Swell1 overexpression significantly reduced infarction size that was expressed as the ratio of infarcted area/total area of the TTC-stained brain slices (0.42 for Cre-Swell1 mice and 0.22 for Cre-EGFP mice). Accordingly, Swell1 overexpression substantially attenuated tMCAO-induced neurological deficits, reflected by improved neurological score (2.00 for Cre-Swell1 mice, 1.25 for Cre-EGFP mice) (Fig. 2B) and longer retaining time on the Rota rod (252.4s for Cre-Swell1 mice, 146.8s for Cre-EGFP mice) (Fig. 2C) in Cre-Swell1 mice. These findings demonstrated that overexpression of Swell1 in microglia significantly decreased ischemic brain damage and ameliorated neurological impairment.

We next examined the effect on microglial Swell1 overexpression on neuronal apoptosis in the ischemic brain using TUNEL and NeuN co-immunostaining on a 10 um-thick brain section that was 3-4 mm way from the frontal tip of olfactory bulb. The hemispheric ratios of the TUNEL (red) and NeuN (green) fluorescence intensity were quantitated to evaluate the overall changes in apoptotic cell death and neuronal loss in the ischemic brain regions of Cre-EGFP and Cre-Swell1 mice. Our data showed that tMCAO induced an approximately 3-fold increase of TUNEL fluorescence intensity and ~1-fold reduction in neuronal loss in the ischemic hemisphere compared to non-ischemic hemisphere, and these changes were significantly suppressed by Swell1 overexpression (Fig. 2D and 2E). To visualize the above change more clearly, we chose an ischemic area that showed mature infarction (area 1, no TTC staining at all) in Cre-EGFP mice, but non-mature infarction (area 3, weak TTC staining) in Cre-Swell1 mice and checked TUNEL staining and neuronal loss under a microscope. Under an enlarged scope, Swell1 overexpression

led to reduced TUNEL-positive cells and alleviated neuronal loss in the ischemic brain region, compared to the corresponding area of the nonischemic hemisphere (area 2 and area 4) (Fig. 2F). These results indicated that overexpression of Swell1 in microglia reduced ischemic brain damage and improved neurological function by inhibiting neuronal apoptosis.

Swell1 overexpression promotes M2 polarization of microglia and reduces inflammation after ischemic stroke

We next examined how microglial Swell1 overexpression is neuroprotective in ischemic stroke and investigated its effect on the polarization of microglia and the production of inflammatory cytokines in vivo and in vitro. The expression of inflammatory cytokines (including IL-1β, IL-4, IL-6, IL-10, IL-12, MCP-1, MIP-1α, MIP-1β, TNF-α, IFN-γ) of both the tissue and the serum in Cre-Swell1 mice and Cre-EGFP mice were measured by Bio-Plex Pro Mouse Chemokine Assay after subjected to tMCAO. The data demonstrated that the expression of most inflammation-related factors in the ischemic area (IA) was significantly higher than that in the non-ischemic area (NA) after ischemic stroke (except IL-4,IL-10 in Cre-EGFP mice and IL-12,TNF-α in Cre-Swell1 mice), and the expression of M1-associated inflammatory factor including IL-1, IL-6, MIP-1α, MIP-1β, TNF-α, IFN-γ in the IA of the Cre-Swell1 mice was significantly decreased compared with the Cre-EGFP mice, but the expression of M2-associated IL-4 and IL-10 was markedly increased, and there were no significant changes in the expression of IL-12 and MCP-1 (Fig.3A). Furthermore, the results of serum sample showed that the levels of inflammation-related factors above in Cre-Swell1 mice were also significantly lower than those in Cre-EGFP mice except for IL-4 and IL-10and these two factors were notably higher than that in Cre-EGFP mice, which was consistent with the results of brain tissue sample (Fig.3B).

To further explore the above effect of microglia Swell1 on microglial polarization in vitro, we detected the expression levels of mRNA and protein of inflammation-related factors by ELISA and Real Time-PCR in BV2 cells with OGD treatment. The data showed that OGD induced notably upregulation of IL-1β, IL-6 and TNF-α protein expression, and knockdown of Swell1 significantly further elevated these increases, whereas overexpression of Swell1 significantly inhibited these change (Fig.3C). Interestingly, only Swell1 overexpression increased the protein level of IL-10 in BV2 cells after OGD, while knockdown of Swell1 induced up-regulation of IL-1β, IL-6 and TNF-α proteins in the normal condition (Normal group) (Fig.3C) and Swell1 overexpression and knockdown has the same effect as protein data on the regulation of above gene transcription level (Fig.3D). Next, we have also tested the transcription level of M2-associated gene Arg-1, CD206 and M1-associated gene CD86. The results demonstrated that the gene expression of Arg-1 and CD206 were significantly downregulated and that of CD86 was obviously upregulated induced by OGD, and knockdown of Swell1 exacerbated this effect, but overexpression of Swell1 can reverse this change (Fig.3D).

In order to verify the effect of Swell1 overexpression in microglia on neuron survival in vitro, we conducted indirect co-culture system with BV2 cells and HT22 cells (work flow seen Fig.3E). After OGD treatment, the data demonstrated that the culture medium produced from BV2 cells transfected with Ad-

Swell1 (Ad-Swell1-MCM) significantly promoted cell survival compared with medium transfected with control adenovirus (vec-MCM) (Fig.3E). This result suggests that overexpression of Swell1 in microglia can promote neuron survival which related to its function of inducing M2 polarization after ischemic stroke. Collectively, these findings suggest that Swell1 overexpression induces microglia M2 polarization to reduce inflammation and promote neuron survival under ischemic condition.

Swell1 overexpression promotes microglia survival after ischemic stroke both in vivo and in vitro

Although polarized microglia have a dual role in inflammation, selective ablation of proliferating microglial exacerbates ischemic injury after stroke[10,30]. Apart from proved role of elevating M2 polarization induced by overexpression of Swell1, we next determined whether the effect of Swell1 overexpression on microglia polarization was based on regulating microglia survival after ischemic stroke. Firstly, co-immunostaining Swell1-FITC (or EGFP), TMEM119-Cy5 (microglia specific biomarker) and DAPI (for nucleus) were performed on the coronal brain slices of Cre-EGFP and Cre-Swell1 mice after subjected to tMCAO. Our data showed that tMCAO induced an approximately 50% reduction of TMEM119 fluorescence intensity in the ischemic hemisphere compared to non-ischemic hemisphere, and this change were significantly reversed by Swell1 overexpression (Fig.4A and B), meanwhile, under an enlarged view, Swell1 overexpression led to increased TMEM119-postive microglia in the ischemic brain region (area 1and area 3, the selected areas were the same as Fig. 2F) compared to the corresponding area of the nonischemic brain hemisphere (area 2 and area 4) (Fig. 4C).

To further analyze whether Swell1 affects the survival of BV2 cells in vitro, cell viability was assessed by CCK-8 assay after OGD treatment. Pretreatment with Swell1 siRNA (Fig. 4D) and DCPIB (Fig. 4E) both aggravated the decrease of living cells induced by OGD treatment, while overexpression of Swell1 increased the number of survivals BV2 cells (Fig.4D). We further examined the effect of Swell1 on the apoptosis and proliferation of BV2 cells using flow cytometry after ischemia. As shown in Fig. 4F and 4G, OGD challenge remarkably increased the early apoptotic rate of BV2 cells (approximately 1.6-fold) compared with the con-Normal group, which was significantly inhibited by Swell1 overexpression but further escalated by Swell1 silencing, respectively. Moreover, it has been proven that the partially survived microglia will be activated and entered the mitotic cycle after OGD treatment[5,31], so we examined that whether Swell1 participated in OGD-induced BV2 cells proliferation. As shown in Fig. 4H and 4I, OGD treatment promoted BV2 cell cycle transition from G0/G1 phase to S phase (suggested more cells were undergoing mitosis) and Swell1 silencing markedly inhibited BV2 cell cycle transition, and conversely Swell1 overexpression further significantly potentiated this transition induced by OGD treatment. Taken together, these results revealed that overexpression of Swell1 protected the survival of microglia through inhibiting apoptosis and promoting proliferation after ischemic stroke.

Swell1 overexpression protects microglia survival through activating SGK1 signaling pathway

In our previous studies, we demonstrated that VRAC opening can induce the outflow of intracellular solute, the decreased intracellular Cl^-, other than Na^+ or K^+, which is responsible for the increased

phosphorylation of SGK1 to inhibit cell apoptosis[24]. So, we hypothesized that the efflux of Cl^- caused by Swell1 opening can activate the Cl^--sensitive kinase SGK1 and further regulate microglia survival. In order to investigate how Swell1 protected against microglia injury through protein phosphorylation modification, 4D Phosphoproteomics and western-blot assay were performed. As shown in Fig.5A, activation of Swell1 by hypotonicity caused changes in the phosphorylation levels of a variety of proteins associated with cell survival such as SGK1, Bnip3 and FOXO3a. We also verified the effect of Swell1 opening on phosphorylation activation of SGK1 by western-blot, and found that Swell1 knockdown blunted the increased phosphorylation of SGK1 induced by hypotonicity, whereas Swell1 overexpression further strengthen this increase (Fig.5B and C). It has been reported that SGK1 regulates transcription factors such as CREB, NF-κB, FOXO3a, p53 and AP-1, among which CREB and FOXO3a are closely related to cell survival[32]. The phosphorylation of CREB at Ser133 residues induces transcription of cell growth-related genes, while the phosphorylation of FOXO3a inhibits its translocation from the cytoplasm to the nucleus, causes destruction of FOXO3a-dependent transcription, cell cycle arrest and apoptosis[24,33]. In our experiment, the activation of CREB and FOXO3a by Swell1 overexpression is consistent with that of SGK1, which can enhance the increased phosphorylation of CREB and FOXO3a in hypotonicity condition, whereas knockdown of Swell1 inhibited these proteins phosphorylation activation (Fig.5B, C).

To further verify this result, we overexpressed Swell1 in BV2 cells combined with and without the SGK1 inhibitor GSK650394, then exposed to OGD for 1 h. The viability rate of BV2 cells was evaluated by CCK-8 assay and the cell apoptosis rate and cell cycle transition were analyzed by flow cytometry. As shown in Fig.6A, GSK650394 alone can significantly decrease living cells, and overexpression of Swell1 notably increased BV2 cell viability compared with vector control group, while the simultaneous administration of GSK650394 eliminated this effect of Swell1 overexpression under both Normal and OGD condition. Consistency, the results of Flow cytometry also shown that overexpression of Swell1 can significantly inhibited BV2 cells apoptosis and promote cell cycle transition from G0/G1 phase to S phase induced by OGD treatment, while inhibition of SGK1 by GSK650394 obviously hindered these effects of Swell1 (Fig.6B-E).

Swell1 overexpression activates CCCs to promote microglial M2-polarization through WNK/SPAK/ OSR1 kinase network in ischemic stroke

In addition of SGK1 signaling pathway, we also found that the phosphorylation protein modification level of another Cl^--sensitive signaling pathway WNK1-SPAK/OSR1-CCCsregulated by Swell1 in BV2 cells. Recent studies have shown that in the case of decreasing intracellular Cl^- concentration, WNK1 function is identified as a negative regulator of the NLRP3 inflammasome in macrophage through autophosphorylated, then proceeds to phosphorylate its downstream targets SPAK/OSR1, which activate CCCs to restore ion concentrations as well as inhibit further Cl^- efflux[34-39]. NKCC1 (SLC12A2) are the major Cl^- entry transporter among CCCs (SLC12) gene family, it can regulate cell volume and maintain cell homeostasis after osmotic and oxidative stress[40]. Interfering with SLC12A2 expression or function in phagocytes resulted in a significant increase in apoptotic corpse uptake and induced the typical anti-

inflammatory program switch to pro-inflammatory and oxidative stress-related gene programs[26]. As Fig.7A shown that activation of the Swell1 channel on BV2 cells by hypotonic stimulation increased the phosphorylation level of WNK1-SPAK/OSR1-CCCs. The result of western blot also shown that overexpression of Swell1 can further significantly increased the phosphorylation protein level of WNK1-SPAK/OSR1-NKCC1 pathway induced by hypotonic, but interference with Swell1 can inhibited this effect (Fig.7B, C).

To investigate whether the WNK1 was involved in the effect of Swell1 on microglia inflammation and M2-polarization in ischemia stroke, we assessed the WNK463 (a selective pan WNK kinases inhibitor) on BV2 cells treated with adenovirus of overexpressed Swell1 after OGD treatment by ELISA and Real Time-PCR. We first observed a significant M1-polarization of BV2 cells as evidenced by increased IL1-β, IL-6, TNF-α protein level and decreased IL-10 protein level in the presence of WNK463 compared with the control (under OGD condition) using ELISA. The data showed that there was a significant M2-polarization evidenced by decreased protein expression of IL1-β, IL-6, TNF-α and increased protein expression of IL-10 in the Swell1 overexpression group after OGD, but this effect of Swell1 would be significantly blocked by WNK463 (Fig.8A). We had further tested the transcription level of M2-associated genes such as IL-10, Arg-1, CD206 and M1-associated genes including IL-1β, TNF-α and CD86 by Real Time-PCR. Consented with the results of ELISA, WNK463 induced significant BV2 cells M1-polarization evidenced by gene expression of IL-10, Arg-1 and CD206 were significantly downregulated and that of IL-1β, TNF-α, CD86 was obviously upregulated compared with the control (under OGD condition), and prevented Swell1 from promoting M2-polarization of BV2 cells at the transcriptional level (Fig.8B). Collectively, Swell1 may also regulate the WNK1-SPAK/OSR1-NKCC1 signal pathway, thereby promoting microglia M2-polarization and improving the inflammatory microenvironment after ischemic stroke.

Discussion

Our research has demonstrated that Swell1 is an essential component of microglia VRAC and is upregulated in response to ischemic stroke. Moreover, we show that microglial Swell1 overexpression attenuates ischemia-induced neuroinflammation and neural damage, and these effects are mainly mediated by Swell1-activated Cl^--sensitive mechanisms that promote microglial survival and M2-polarization through activating SGK1-FOXO3a/CREB and WNK1-SPAK /OSR1-SLC12A2 signaling pathways.

VRAC has long been considered to regulate the homeostasis of cell volume, cell survival, the release of hormones, and the neurotransmitters like glutamate and aspartate[41,42]. The recent progresses in the identification of Swell1 as an essential VRAC subunit and in the elucidation of the channel structure have made it possible to conduct genetic studies and synthesize specific inhibitors. As of now, the functional significance of Swell1 is still far from understood. Recent studies have shown that Swell1 is closely related to glutamate release, cGAMP trafficking, β-cell excitability and insulin secretion, vascular endothelial function and skeletal muscle differentiation[16,43–45]. However, the role of Swell1-mediated VRAC in stroke is rather puzzling. On the one hand, Swell1 contributes to the non-vesicular release of

glutamate and promotes excitotoxic neural cell death after stroke, and on the other hand, Swell1 promotes the volume recovery of swollen neurons, reduces brain edema, and promotes the survival of neurons following ischemic stroke[46]. Here our data demonstrate that Swell1 is the essential component of VRAC in microglia and is neuroprotective via promoting microglial survival and M2 polarization after ischemic stroke.

The clearance of apoptotic cells is a part of the anti-inflammatory response of phagocytes, but the mechanism behind this response is still being determined[13]. K^+ and Cl^- efflux are critical steps for inflammation activation by stress stimuli, and the Cl^--sensing signal pathway has been reported to be involved in controlling the phagocytosis and anti-inflammatory response of phagocytes[26]. Microglia are the main phagocytes in the brain that clear apoptotic cells after ischemic stroke In a transient ischemic stroke model, activated microglia were found to accumulate in the infarct core area within 24 hours, while in the peri-infarct region, the microglia appeared at a much earlier time point and peaked at 7 days post-reperfusion[31]. Moreover, activated microglia mainly express M2 phenotypic markers in the acute stage, but they gradually switch toward M1 phenotype as the duration of cerebral ischemia extends, and at this point, the microglia start to produce chemokines, which attracts a large number of inflammatory cells to accumulate in the necrotic site[47]. Using a transgenic mouse strain with microglial Swell1 overexpression, here we investigated the role of Swell1-mediated VRAC in microglia distribution and phenotypic transformation following tMCAO in mice. Our data show that Swell1 overexpression not only increases the accumulation of microglia in the ischemic hemisphere, but also promotes its M2-polarization, leading to suppressed neural and systemic inflammatory responses and improved neuron survival and neurological function.

In this study, we observed a drastic reduction of IL-1β level in ischemic brain tissue and in the serum collected from the Swell1 cKI mice after tMCAO, supporting an important role of microglial Swell1 in mediating ischemia-induced neuroinflammation. It is known that the maturation and release of IL-1β is mainly regulated by the NLRP3 inflammasome, and this process is closely associated with Cl^- efflux[37,38]. To our surprise, our data shown that Swell1 overexpression increased the expression of NLRP3 in normal condition and this increase can be blocked by SGK1 inhibitor GSK650394, however overexpression of Swell1 do not further augmented OGD-induced expression of NLRP3 (Fig.S3, 4). These data indicate that Swell1 overexpression itself may lead to maximal NLRP3 activation in microglia, which cannot be further increased under OGD conditions, and the regulation of Swell1 on the secretion of IL-1β in ischemic condition may be through other pathways[18]. Moreover, our data show that the levels of MIP-1α and MIP-1β in the ischemic brain tissue and the serum of Swell1 cKI mice are significantly reduced, and even the level of MCP-1 in the serum is also reduced. We think that the regulation of Swell1 on the secretion of these chemokines may be attributed to its direct action on microglia or to its indirect suppression on inflammatory response of other cells secondary to M2 polarization of microglia that improves the overall inflammatory microenvironment of the ischemic brain region. The resultant immuno-suppressing microenvironment will likely reduce the recruitment of peripheral cells such as neutrophils and

macrophages to the ischemic brain region, and thus attenuating inflammatory brain injury and improving systemic inflammatory response (Figure S5).

Microglia-associated inflammation after ischemic stroke not only relies on its inflammatory phenotype, but also rests with its number and distribution. Reactive microgliosis after ischemic brain injury is typically characterized by a stepwise response, starting with microglial activation, followed by massive expansion and migration of the resident microglial population and the recruitment of bone marrow-derived macrophages that migrate into the neuronal parenchyma and act like microglia[48,49]. Previous stroke studies have shown that survived resident microglia are important for the regulation of neuroinflammation and have an important neuroprotective potential by serving as an endogenous pool of neurotrophic and antiapoptotic molecules such as IGF-1[50,51]. Our previous study showed that VRAC could regulate cell proliferation, apoptosis and survival through the Cl^--sensitive SGK1 signaling pathway[24,52]. To become functional, the SGK1 protein requires activation by phosphorylation, and then further phosphorylates a number of transcription factors[32]. Here, our data show that Swell1 overexpression promotes the accumulation of microglia in the ischemic brain region through inhibiting the apoptosis of resident microglia and promoting their proliferation via activating SGK1 -CREB-FOXO3a pathways.

Conclusions

In conclusion, our findings have shown that Swell1 is an essential component of microglia VRAC and its activation has a protective effect on brain damage and improves post-ischemic neurological outcomes by reducing ischemia-induced inflammation. This work highlights the role of Swell1 in promoting microglial survival and M2 polarization, and thus provides new light for the treatment of neuroinflammation-related ischemic brain injury.

Abbreviations

VRAC	Volume-regulated Cl^- currents
tMCAO	transient middle cerebral artery occlusion
RVD	regulation of volume reduction
OGD	oxygen-glucose deprivation
CCCs	Cation-Chloride Cotransporters
TTC	2, 3, 5-Triphenyltetrazolium chloride
Hypo	Hypotonic
ISO	Isotonic
MOI	multiplicity of infection
cKI	microglia conditional knock-in

Declarations

Availability of data and materials

The datasets used or analyzed during the current study are available from the corresponding author on reasonable request.

Acknowledgements

Not applicable.

Funding

This work was supported by National Natural Science Foundation of China (82003748,81873747,81760227);Natural Science Foundation of Guangdong Province(2019A1515010311);and Shenzhen Science and Technology Innovation Commission (GJHZ20190820115001765, JCYJ20210324115601005) and Guangdong Innovation Platform of Translational Research for Cerebrovascular Diseases.

Author Contribution

Wenlan Liu and Baoyi Chen designed the study; Wenlan Liu, Baoyi Chen and Yuan Zhang wrote the manuscript; Baoyi Chen, Cong Xie, Tengrui Shi and Shiqin Yue performed the experiments; Baoyi Chen and Cong Xie analyzed the data; Wenlan Liu, Yuan Zhang, Weiping Li and Guodong Huang revised the manuscript; Wenlan Liu and Yuan Zhang are the guarantors of this work. All authors read and approved the final manuscript.

Ethics declarations

Ethics approval and consent to participate: All animal procedures were conducted in accordance with the Guidelines for Care and Use of Laboratory Animals of Shenzhen University and all efforts were made to minimize animal suffering. The study protocol was approved by the Ethics Committee of the First Affiliated Hospital of Shenzhen University.

Consent for publication: All authors concur with the submission.

Competing interests: The authors declare that they have no competing interests.

References

1. Campbell, B. C. V.*et al.* Ischaemic stroke. *Nat Rev Dis Primers* **5**, 70, doi:10.1038/s41572-019-0118-8 (2019).
2. Lipton, P. Ischemic cell death in brain neurons. *Physiol Rev* **79**, 1431-1568, doi:10.1152/physrev.1999.79.4.1431 (1999).

3. Iadecola, C. & Anrather, J. The immunology of stroke: from mechanisms to translation. *Nat Med* **17**, 796-808, doi:10.1038/nm.2399 (2011).
4. Fu, Y., Liu, Q., Anrather, J. & Shi, F. D. Immune interventions in stroke. *Nat Rev Neurol* **11**, 524-535, doi:10.1038/nrneurol.2015.144 (2015).
5. Kim, E. & Cho, S. Microglia and Monocyte-Derived Macrophages in Stroke. *Neurotherapeutics* **13**, 702-718, doi:10.1007/s13311-016-0463-1 (2016).
6. Petrovic-Djergovic, D., Goonewardena, S. N. & Pinsky, D. J. Inflammatory Disequilibrium in Stroke. *Circ Res* **119**, 142-158, doi:10.1161/CIRCRESAHA.116.308022 (2016).
7. Ma, Y., Wang, J., Wang, Y. & Yang, G. Y. The biphasic function of microglia in ischemic stroke. *Prog Neurobiol* **157**, 247-272, doi:10.1016/j.pneurobio.2016.01.005 (2017).
8. Hu, X.*et al.* Microglial and macrophage polarization-new prospects for brain repair. *Nat Rev Neurol* **11**, 56-64, doi:10.1038/nrneurol.2014.207 (2015).
9. Lyu, J.*et al.* Microglial/Macrophage polarization and function in brain injury and repair after stroke. *CNS Neurosci Ther* **27**, 515-527, doi:10.1111/cns.13620 (2021).
10. Lalancette-Hebert, M., Gowing, G., Simard, A., Weng, Y. C. & Kriz, J. Selective ablation of proliferating microglial cells exacerbates ischemic injury in the brain. *J Neurosci* **27**, 2596-2605, doi:10.1523/JNEUROSCI.5360-06.2007 (2007).
11. Rudolph, M.*et al.* Microglia-mediated phagocytosis of apoptotic nuclei is impaired in the adult murine hippocampus after stroke. *Glia* **69**, 2006-2022, doi:10.1002/glia.24009 (2021).
12. Salter, M. W. & Stevens, B. Microglia emerge as central players in brain disease. *Nat Med* **23**, 1018-1027, doi:10.1038/nm.4397 (2017).
13. Arandjelovic, S. & Ravichandran, K. S. Phagocytosis of apoptotic cells in homeostasis. *Nat Immunol* **16**, 907-917, doi:10.1038/ni.3253 (2015).
14. Rungta, R. L.*et al.* The cellular mechanisms of neuronal swelling underlying cytotoxic edema. *Cell* **161**, 610-621, doi:10.1016/j.cell.2015.03.029 (2015).
15. Hoffmann, E. K., Lambert, I. H. & Pedersen, S. F. Physiology of cell volume regulation in vertebrates. *Physiol Rev* **89**, 193-277, doi:10.1152/physrev.00037.2007 (2009).
16. Lahey, L. J.*et al.* LRRC8A:C/E Heteromeric Channels Are Ubiquitous Transporters of cGAMP. *Mol Cell* **80**, 578-591 e575, doi:10.1016/j.molcel.2020.10.021 (2020).
17. Qiu, Z.*et al.* SWELL1, a plasma membrane protein, is an essential component of volume-regulated anion channel. *Cell* **157**, 447-458, doi:10.1016/j.cell.2014.03.024 (2014).
18. Green, J. P.*et al.* LRRC8A is essential for hypotonicity-, but not for DAMP-induced NLRP3 inflammasome activation. *Elife* **9**, doi:10.7554/eLife.59704 (2020).
19. Voss, F. K.*et al.* Identification of LRRC8 heteromers as an essential component of the volume-regulated anion channel VRAC. *Science* **344**, 634-638, doi:10.1126/science.1252826 (2014).
20. Zhou, J. J.*et al.* LRRC8A-dependent volume-regulated anion channels contribute to ischemia-induced brain injury and glutamatergic input to hippocampal neurons. *Exp Neurol* **332**, 113391,

doi:10.1016/j.expneurol.2020.113391 (2020).

21. Yang, J.*et al.* Glutamate-Releasing SWELL1 Channel in Astrocytes Modulates Synaptic Transmission and Promotes Brain Damage in Stroke. *Neuron* **102**, 813-827 e816, doi:10.1016/j.neuron.2019.03.029 (2019).
22. Li, P.*et al.* LRRC8 family proteins within lysosomes regulate cellular osmoregulation and enhance cell survival to multiple physiological stresses. *Proc Natl Acad Sci U S A* **117**, 29155-29165, doi:10.1073/pnas.2016539117 (2020).
23. Serra, S. A.*et al.* LRRC8A-containing chloride channel is crucial for cell volume recovery and survival under hypertonic conditions. *Proc Natl Acad Sci U S A* **118**, doi:10.1073/pnas.2025013118 (2021).
24. Chen, B. Y.*et al.* SGK1 mediates the hypotonic protective effect against H2O2-induced apoptosis of rat basilar artery smooth muscle cells by inhibiting the FOXO3a/Bim signaling pathway. *Acta Pharmacol Sin* **41**, 1073-1084, doi:10.1038/s41401-020-0357-y (2020).
25. Zhang, Y. J.*et al.* WNK1 is required for proliferation induced by hypotonic challenge in rat vascular smooth muscle cells. *Acta Pharmacol Sin* **39**, 35-47, doi:10.1038/aps.2017.56 (2018).
26. Perry, J. S. A.*et al.* Interpreting an apoptotic corpse as anti-inflammatory involves a chloride sensing pathway. *Nat Cell Biol* **21**, 1532-1543, doi:10.1038/s41556-019-0431-1 (2019).
27. Longa, E. Z., Weinstein, P. R., Carlson, S. & Cummins, R. Reversible middle cerebral artery occlusion without craniectomy in rats. *Stroke* **20**, 84-91, doi:10.1161/01.str.20.1.84 (1989).
28. Jin, X.*et al.* Spatiotemporal evolution of blood brain barrier damage and tissue infarction within the first 3h after ischemia onset. *Neurobiol Dis* **48**, 309-316, doi:10.1016/j.nbd.2012.07.007 (2012).
29. Sumida, T.*et al.* Activated beta-catenin in Foxp3(+) regulatory T cells links inflammatory environments to autoimmunity. *Nat Immunol* **19**, 1391-1402, doi:10.1038/s41590-018-0236-6 (2018).
30. Zhang, Q.*et al.* Cell cycle inhibition attenuates microglial proliferation and production of IL-1beta, MIP-1alpha, and NO after focal cerebral ischemia in the rat. *Glia* **57**, 908-920, doi:10.1002/glia.20816 (2009).
31. Gelderblom, M.*et al.* Temporal and spatial dynamics of cerebral immune cell accumulation in stroke. *Stroke* **40**, 1849-1857, doi:10.1161/STROKEAHA.108.534503 (2009).
32. Lang, F.*et al.* (Patho)physiological significance of the serum- and glucocorticoid-inducible kinase isoforms. *Physiol Rev* **86**, 1151-1178, doi:10.1152/physrev.00050.2005 (2006).
33. David, S. & Kalb, R. G. Serum/glucocorticoid-inducible kinase can phosphorylate the cyclic AMP response element binding protein, CREB. *FEBS Lett* **579**, 1534-1538, doi:10.1016/j.febslet.2005.01.040 (2005).
34. Alessi, D. R.*et al.* The WNK-SPAK/OSR1 pathway: master regulator of cation-chloride cotransporters. *Sci Signal* **7**, re3, doi:10.1126/scisignal.2005365 (2014).
35. Moriguchi, T.*et al.* WNK1 regulates phosphorylation of cation-chloride-coupled cotransporters via the STE20-related kinases, SPAK and OSR1. *J Biol Chem* **280**, 42685-42693,

doi:10.1074/jbc.M510042200 (2005).

36. Huang, H.*et al.* The WNK-SPAK/OSR1 Kinases and the Cation-Chloride Cotransporters as Therapeutic Targets for Neurological Diseases. *Aging Dis* **10**, 626-636, doi:10.14336/AD.2018.0928 (2019).
37. Clauzure, M.*et al.* NLR family pyrin domain containing 3 (NLRP3) and caspase 1 (CASP1) modulation by intracellular Cl(-) concentration. *Immunology* **163**, 493-511, doi:10.1111/imm.13336 (2021).
38. Mayes-Hopfinger, L.*et al.* Chloride sensing by WNK1 regulates NLRP3 inflammasome activation and pyroptosis. *Nat Commun* **12**, 4546, doi:10.1038/s41467-021-24784-4 (2021).
39. Gagnon, K. B., England, R. & Delpire, E. Characterization of SPAK and OSR1, regulatory kinases of the Na-K-2Cl cotransporter. *Mol Cell Biol* **26**, 689-698, doi:10.1128/MCB.26.2.689-698.2006 (2006).
40. Hebert, S. C., Mount, D. B. & Gamba, G. Molecular physiology of cation-coupled Cl- cotransport: the SLC12 family. *Pflugers Arch* **447**, 580-593, doi:10.1007/s00424-003-1066-3 (2004).
41. Lutter, D., Ullrich, F., Lueck, J. C., Kempa, S. & Jentsch, T. J. Selective transport of neurotransmitters and modulators by distinct volume-regulated LRRC8 anion channels. *J Cell Sci* **130**, 1122-1133, doi:10.1242/jcs.196253 (2017).
42. Osei-Owusu, J., Yang, J., Vitery, M. D. C. & Qiu, Z. Molecular Biology and Physiology of Volume-Regulated Anion Channel (VRAC). *Curr Top Membr* **81**, 177-203, doi:10.1016/bs.ctm.2018.07.005 (2018).
43. Kang, C.*et al.* SWELL1 is a glucose sensor regulating beta-cell excitability and systemic glycaemia. *Nat Commun* **9**, 367, doi:10.1038/s41467-017-02664-0 (2018).
44. Kumar, A.*et al.* SWELL1 regulates skeletal muscle cell size, intracellular signaling, adiposity and glucose metabolism. *Elife* **9**, doi:10.7554/eLife.58941 (2020).
45. Alghanem, A. F.*et al.* The SWELL1-LRRC8 complex regulates endothelial AKT-eNOS signaling and vascular function. *Elife* **10**, doi:10.7554/eLife.61313 (2021).
46. Barros, L. F., Hermosilla, T. & Castro, J. Necrotic volume increase and the early physiology of necrosis. *Comp Biochem Physiol A Mol Integr Physiol* **130**, 401-409, doi:10.1016/s1095-6433(01)00438-x (2001).
47. Schilling, M., Strecker, J. K., Ringelstein, E. B., Schabitz, W. R. & Kiefer, R. The role of CC chemokine receptor 2 on microglia activation and blood-borne cell recruitment after transient focal cerebral ischemia in mice. *Brain Res* **1289**, 79-84, doi:10.1016/j.brainres.2009.06.054 (2009).
48. Priller, J.*et al.* Targeting gene-modified hematopoietic cells to the central nervous system: use of green fluorescent protein uncovers microglial engraftment. *Nat Med* **7**, 1356-1361, doi:10.1038/nm1201-1356 (2001).
49. Stoll, G. & Jander, S. The role of microglia and macrophages in the pathophysiology of the CNS. *Prog Neurobiol* **58**, 233-247, doi:10.1016/s0301-0082(98)00083-5 (1999).
50. Xiong, X. Y., Liu, L. & Yang, Q. W. Functions and mechanisms of microglia/macrophages in neuroinflammation and neurogenesis after stroke. *Prog Neurobiol* **142**, 23-44,

doi:10.1016/j.pneurobio.2016.05.001 (2016).

51. Kim, D. H.*et al.* Early immature neuronal death initiates cerebral ischemia-induced neurogenesis in the dentate gyrus. *Neuroscience* **284**, 42-54, doi:10.1016/j.neuroscience.2014.09.074 (2015).
52. Chen, B. Y.*et al.* SGK1 mediates hypotonic challenge-induced proliferation in basilar artery smooth muscle cells via promoting CREB signaling pathway. *Eur J Pharmacol* **898**, 173997, doi:10.1016/j.ejphar.2021.173997 (2021).

Figures

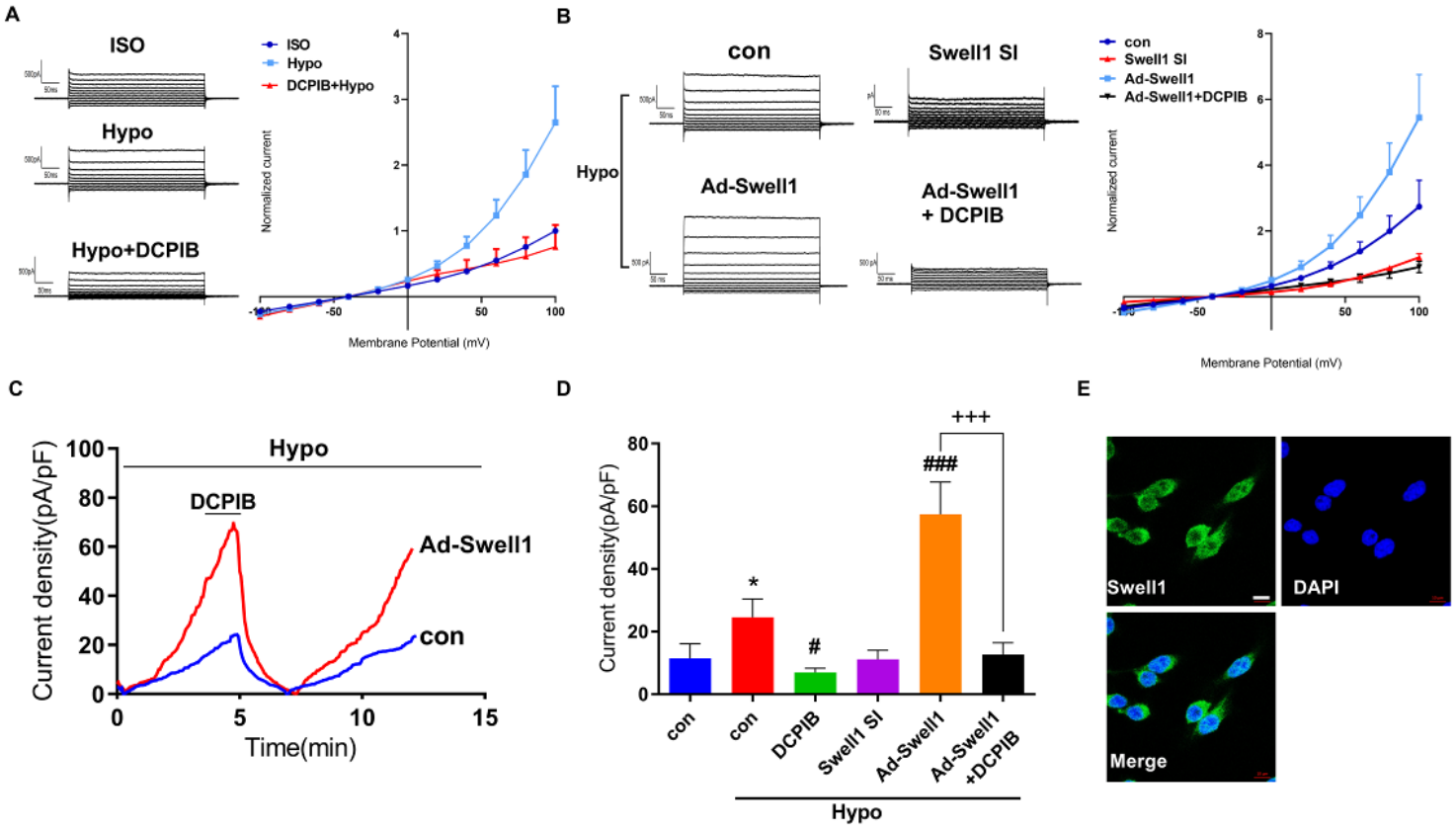

Figure 1

Swell1 is required for microglia VRAC activated and chloride efflux by cell swelling

A, Representative whole-cell currents recorded by voltage step protocols in ISO (300 mOsm/kg) or Hypo (220 mOsm/kg) solution with (or without) DCPIB (50 mM) pretreatment for cultured BV2 (Left). Normalized current-voltage (I-V) curve shows the effect of Hypo solution and DCPIB on chloride currents (Right). n=6

B, Representative whole-cell currents recorded (Left) and Normalized current-voltage (I-V) curve (Right) by voltage step in Hypo solution for cultured control and Swell1 knock-in or knock-down BV2 cells, DCPIB was added as indicated. n=6

C, Time course of whole-cell current densities at +100 mV, induced by Hypo solution for control and Swell1 knock-in BV2 cells, DCPIB was added as indicated. n=6

D, Quantification of current densities at +100 mV activated by Hypo solution. n=6, Mann-Whitney test, *p < 0.05 *vs* con (ISO), $^{\#}$ p < 0.05 *vs*. con (Hypo), $^{\#\#\#}$ p< 0.001 *vs* con (Hypo), $^{+++}$ p< 0.001 *vs*. Ad-Swell1 (Hypo).

E, Images of Swell1 fluorescence stained in BV2 cells. Cell nucleus was stained by DAPI (blue), Swell1 was stained by FITC-labeled antibody (green). n=5, Scale bar: 10μm.

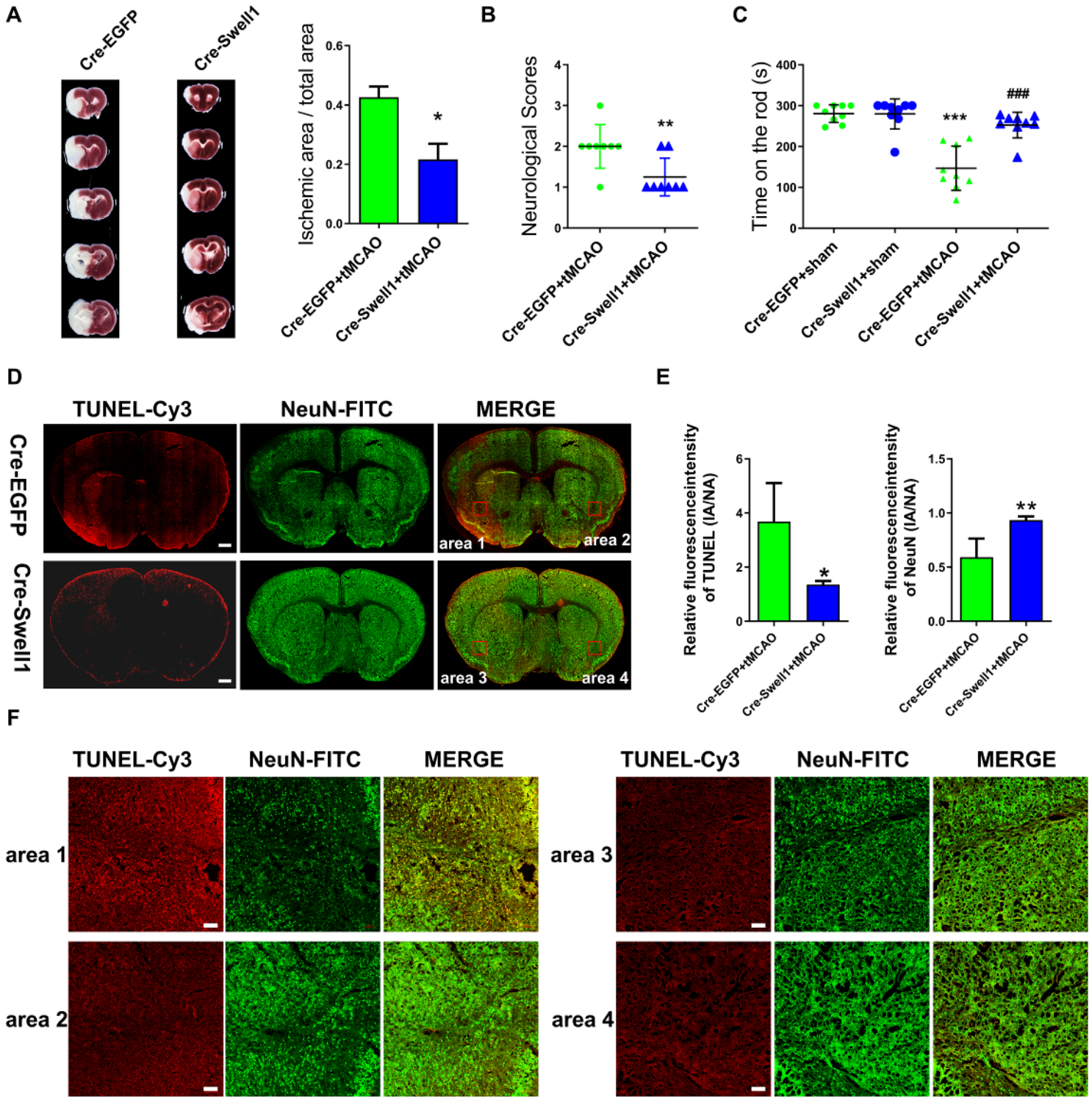

Figure 2

Swell1 cKI (microglia conditional knock-in) mice are protected in ischemic stroke

A, Representative images of triphenyl tetrazolium chloride (TTC) staining in Cre-EGP and Cre-Swell1 mice subjected to tMCAO (Left). Quantification of total infarct area volume ratio (Right). n = 5 for EGFP and Swell1 cKI mice, respectively. Mann Whitney test, *p < 0.05.

B, Quantification of neurological score in mice after subjected to tMCAO. n = 8 for EGFP and Swell1 cKI mice, respectively. Mann-Whitney test, **p < 0.01.

C, Quantification of mice time on the rod before and after subjected to tMCAO in Rota rod system. N=9 for Cre-EGFP and Cre-Swell1 mice, respectively. Tukey's multiple comparisons test, ***p < 0.001, $^{###}$p< 0.001

D, Representative images of whole brain sections fluorescence staining of mice subjected to tMCAO. TUNEL was stained by Cy3 (red), NeuN was stained by FITC (green). Scale bar: 500 μm.

E, Quantification of relative average fluorescence intensity of TUNEL (Left) and NeuN (Right) in ischemic area and non-ischemic area. n = 6 for Cre-EGFP and Cre-Swell1 mice, respectively. Unpaired t test, *p < 0.05, **p < 0.01.

F, Zoom in image shown brain damage in four ischemic and non-ischemic areas, respectively. Scale bar: 100 μm.

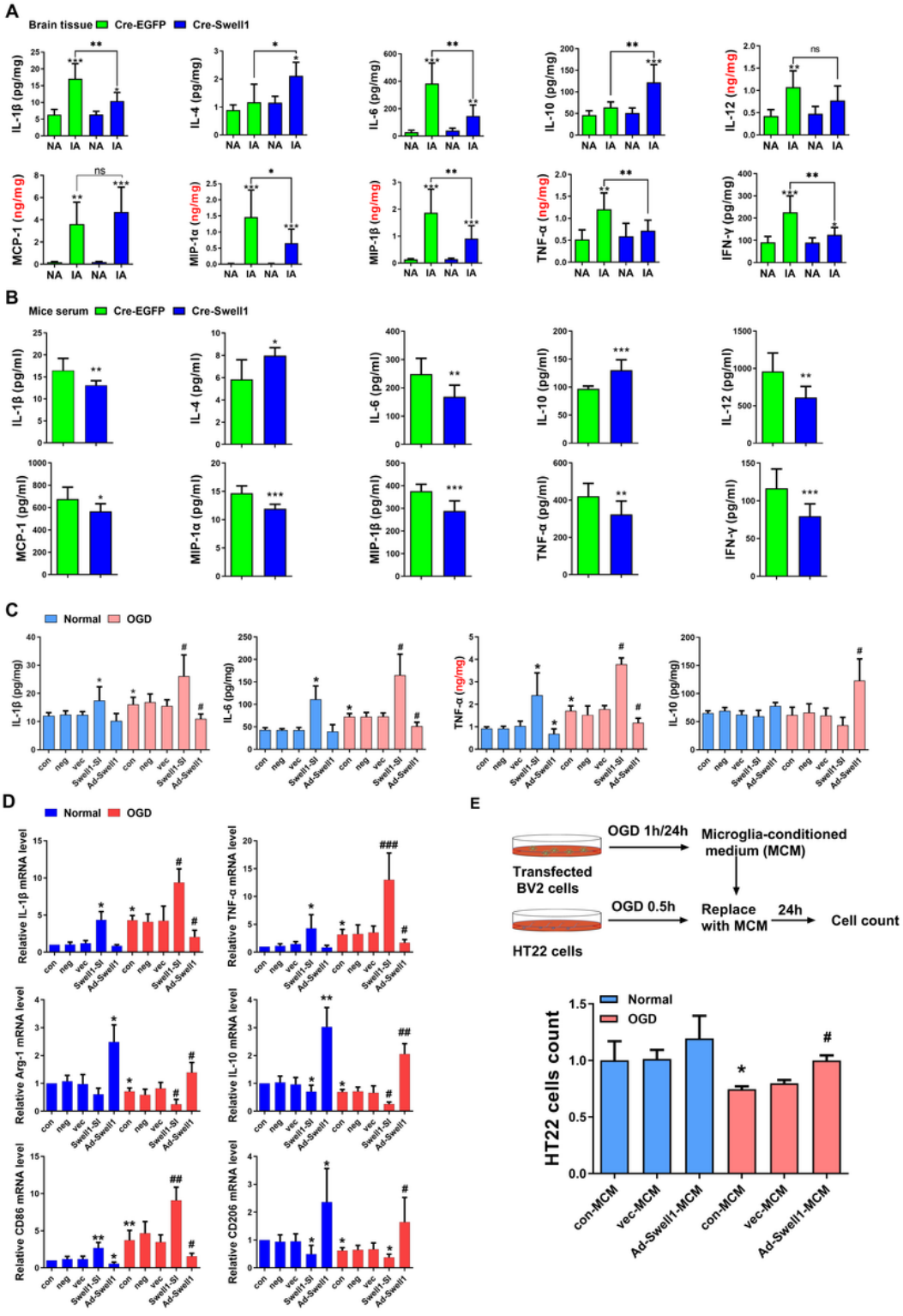

Figure 3

Swell1 promotes M2-polarization of microglia both in vivo and vitro

A and B, Quantification of the inflammation-related cytokines in mice brains (A) and serum (B) after subjected to tMCAO by Bio-Plex Pro Mouse Chemokine Assay. Cellular fractions were prepared from the ischemic area (IA) and the same location of the non-ischemic area (NA). n=8-10 for Cre-EGFP (green) and

Cre-Swell1 (blue) mice, respectively. Unpaired t test, *p<0.05, **p<0.01, ***p<0.001 *vs* Cre-EGFP-IA group (A) or Cre-EGFP group (B).

C and D, BV2 cells were transfected with Swell1 siRNA or Swell1 overexpressed adenovirus, or their negative control for 24 h, and treated with OGD as indicated. The effect of Swell1 on inflammation-related factors IL-1β, IL-6, IL-10 and TNF-α expression was measured by Elisa (C), while the mRNA levels of IL-1β, IL-10, Arg-1, TNF-α, CD86 and CD206was detected by RT-PCR (D). n=6, Tukey's multiple comparisons test, *p<0.05 *vs*. con-Normal, $^{\#}$p<0.05 *vs*. con-OGD.

E, The effect of Ad-Swell1 transfected microglia conditioned medium (MCM) on the HT22 cells survival after OGD. Experimental process diagram (Above) and quantitative analysis of HT22 cell viability (Right) were shown. n=6, Student's t test, *p < 0.05 *vs*. con-normal, $^{\#}$p< 0.05 *vs*. con-OGD.

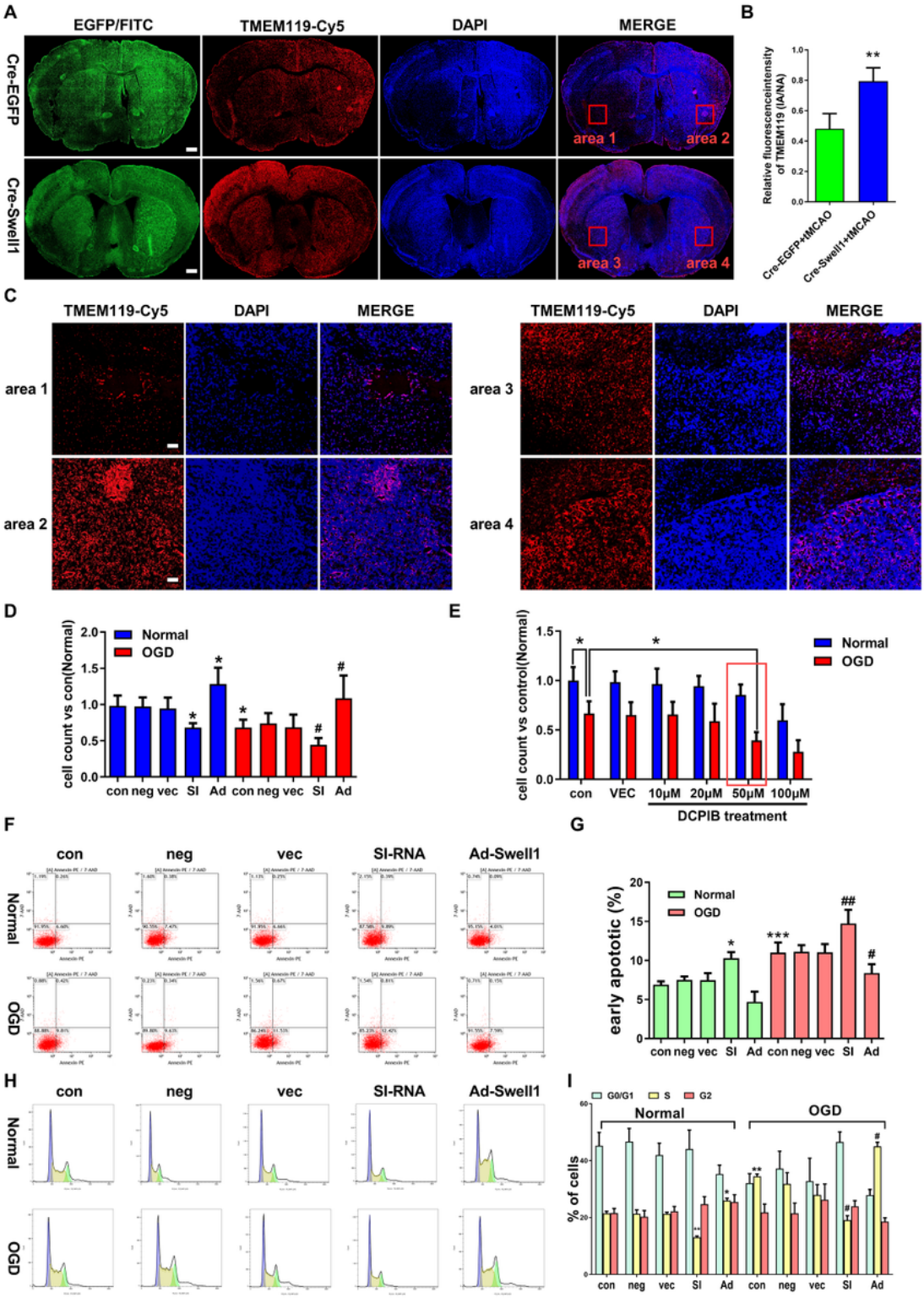

Figure 4

Swell1 promotes microglia survival after ischemic stroke

A, Representative images of whole brain sections fluorescence staining of mice subjected to tMCAO. TMEM119 was stained by Cy5 (red), Swell1 was stained by FITC (green), Cell nucleus was stained by DAPI (blue). Scale bar: 500 μm.

B, Quantification of relative average fluorescence intensity of TMEM119 in ischemic area and non-ischemic area. n = 6 for EGFP and Swell1 cKI mice, respectively. Unpaired t test, **p < 0.01.

C, Zoom in image shows microglia survival in ischemic and non-ischemic areas, Scale bar: 100 μm.

D, BV2 cells were transfected with Swell1 siRNA (Swell1 Si) or Swell1-expressed adenovirus (Ad-Swell1), or their negative control (neg and vec for short, respectively) for 24 h, and then treated with OGD for 1 h, then replace with normal medium for another 24 h. Cell viability were measured by CCK-8 assay and shown in bar charts. n=6, Tukey's multiple comparisons test, *p<0.05 *vs*. con-Normal, $^{\#}$p<0.05 *vs*. con-OGD.

E, BV2 cells are treated with different concentrations of DCPIB, then encountered OGD for 1 h, and replace with normal medium for another 24 h or just no special treatment. Cell viability were measured by CCK-8 assay and shown in bar charts. n=6, Tukey's multiple comparisons test, *p<0.05.

F - I, BV2 cells were transfected with Swell1 siRNA or overexpressed adenovirus as indicate. The effects of Swell1 silence or overexpression on OGD-induced apoptosis (F) and cell cycle transition (H) were measured by flow cytometry. For apoptosis, percentage of early apoptotic cells were quantitatively analyzed (G). For cell cycle transition, percentage of cells in each phase of the cell cycle were shown in bar charts, and S phase were quantitatively analyzed (I). n=6, Tukey's multiple comparisons test, *p<0.05, ***p < 0.001 *vs*. con-Normal, $^{\#}$p<0.05, $^{\#\#}$p<0.01 *vs*. con-OGD, respectively.

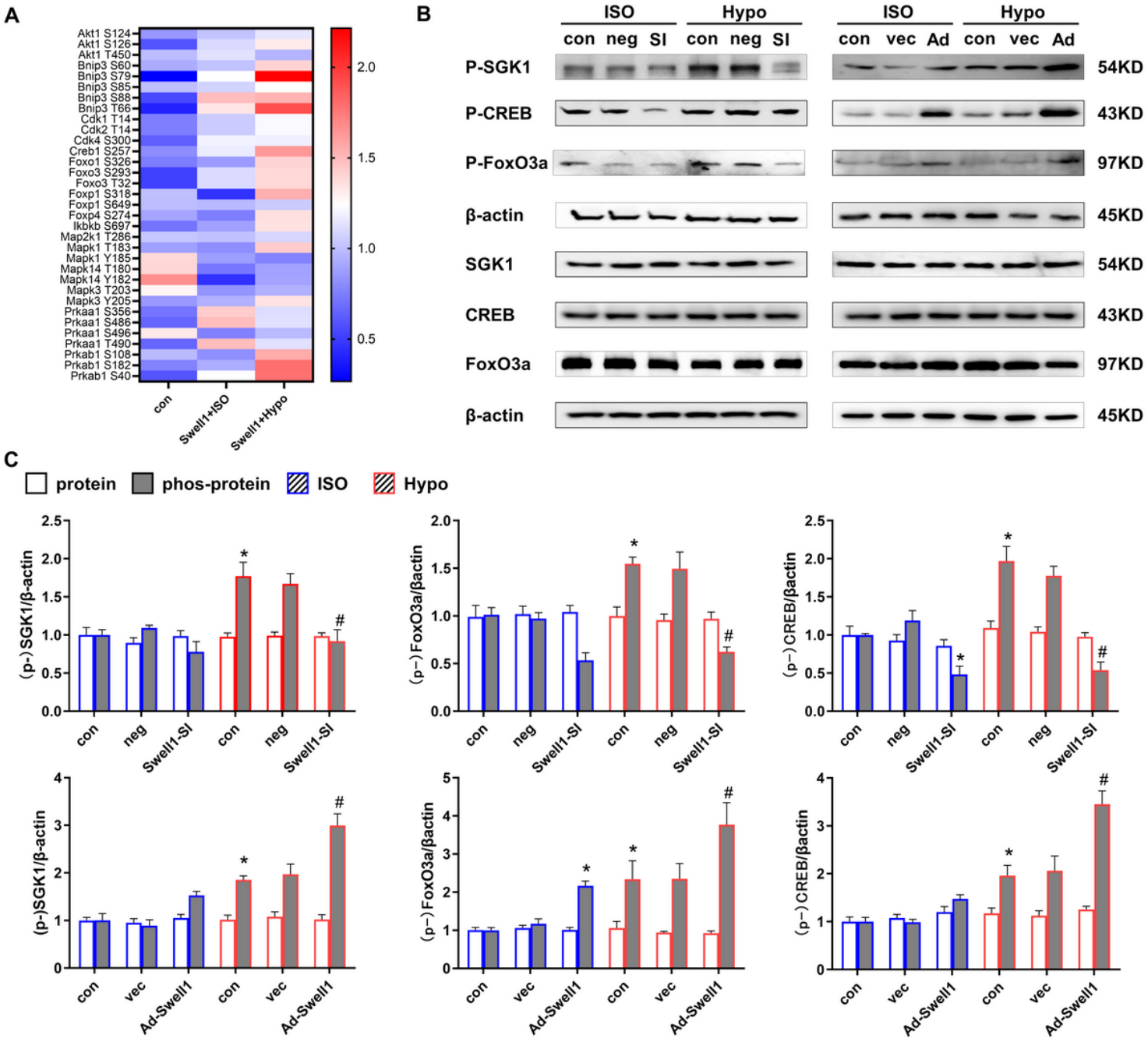

Figure 5

Swell1 opening induced by hypotonicity increases SGK1 activity and activates the CREB/FOXO3a signaling pathway.

A, Heatmap revealing 4D Phosphoproteomics result of Swell1 overexpression on the phosphorylation levels of a variety of proteins associated with cell survival in different treatments. BV2 cells were transfected with Swell1 overexpressed adenovirus for 48 h as indicate, and then incubated in isotonic (ISO) or hypotonic (Hypo) solution for 10min.

B and C, BV2 cells were transfected with Swell1 siRNA or overexpressed adenovirus, or the respective negative control (neg and vec, respectively) as indicate and then incubated in ISO or Hypo solution for 10min, the effects of Swell1 silencing or overexpression on the phosphorylation protein level of SGK1, FOXO3a and CREB in different treatments were measured by western-blot (B). Densitometric analysis of SGK1, FOXO3a and CREB phosphorylation were shown in the bar graphs (C). n = 6, *p < 0.05 *vs*. con - ISO, $^{\#}$p < 0.05 *vs*. con - Hypo.

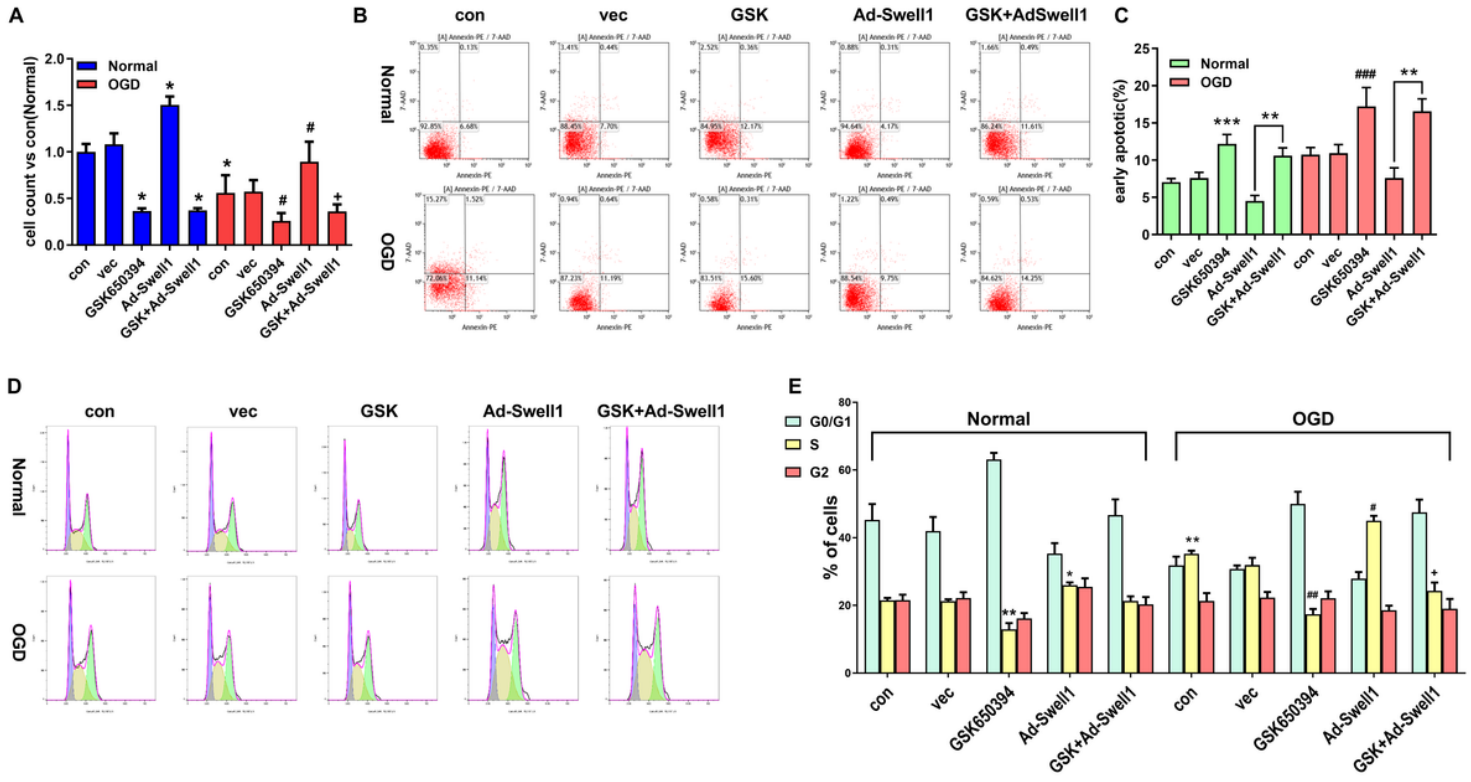

Figure 6

Swell1 protects microglia survival after OGD treatment was hindered by GSK650394.

A-E, BV2 cells were transfected with Swell1 overexpressed adenovirus or (and) just pretreated GSK650394 (100mM) for 6 h before OGD treatment as indicated. Cell viability were measured by CCK-8 assay and shown in bar charts (A). The effects of Swell1 and GSK650394 on OGD-induced apoptosis were measured by flow cytometry, Percentage of early apoptotic cells were quantitatively analyzed (B, C). The effects of Swell1 and GSK650394 on OGD-induced cell cycle transition were measured by flow cytometry, Percentage of cells in each phase of the cell cycle were shown in bar charts, and S phase were quantitatively analyzed (D, E). n=6, Tukey's multiple comparisons test, *p<0.05 *vs*. con-Normal, $^{\#}$p<0.05 *vs*. con-OGD, $^{+}$p<0.05 *vs*. Ad-Swell1-OGD, ** p<0.01 *vs*. con-Normal, $^{\#\#}$ p<0.01 *vs*. con-OGD, $^{\#\#\#}$ p<0.001 *vs*. con-OGD.

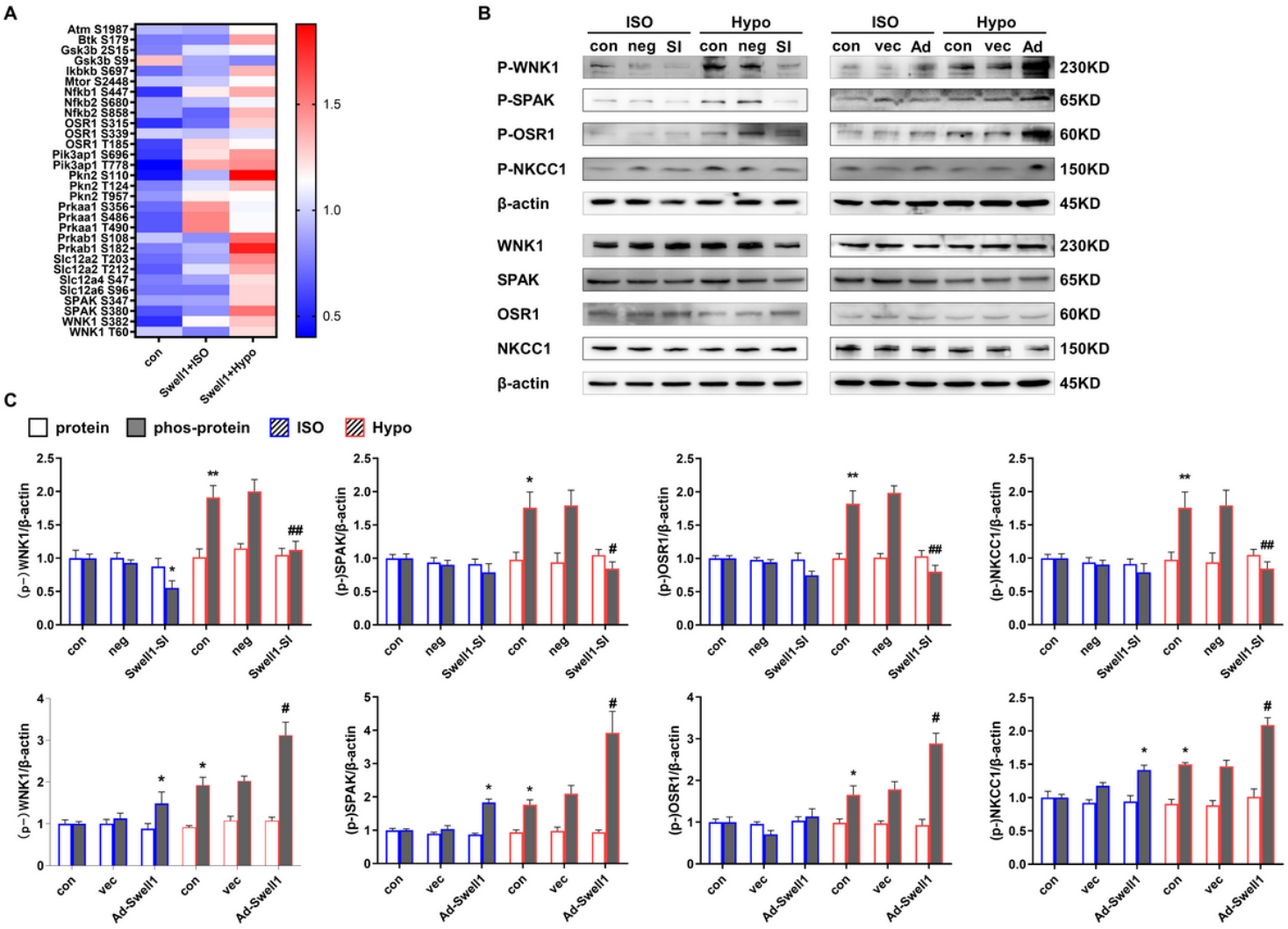

Figure 7

Swell1 channel promotes the phosphorylation of WNK-SPAK/OSR1 kinases and Cation-Chloride Cotransporters.

A, BV2 cells were transfected with Swell1 overexpressed adenovirus for 48 h as indicate, and then incubated in isotonic (ISO) or hypotonic solution (Hypo) for 10min. The effects of Swell1 overexpression on the phosphorylation levels of a variety of proteins associated with inflammation in different treatments were measured by 4D Phosphoproteomics.

B and C, BV2 cells were transfected with Swell1 siRNA or expressed adenovirus or the respective negative control (neg and vec, respectively) as indicate. Cells at 48h post transfection were exposed for 10 min to either control isotonic or hypotonic conditions, the effects of Swell1 silencing or overexpression on the expression and phosphorylation of WNK1, SPAK, OSR1 and NKCC1 in different treatments were measured by western-blot (B). Densitometric analysis of phosphorylation level of WNK1, SPAK, OSR1 and NKCC1 protein was shown in the bar graphs(C). n = 6, Tukey's multiple comparisons test, *p < 0.05 *vs.* con in ISO, $^{\#}$p < 0.05 *vs.* con in Hypo, ** p <0.01 *vs.* con in ISO, $^{\#\#}$ p< 0.05 *vs.* con in Hypo.

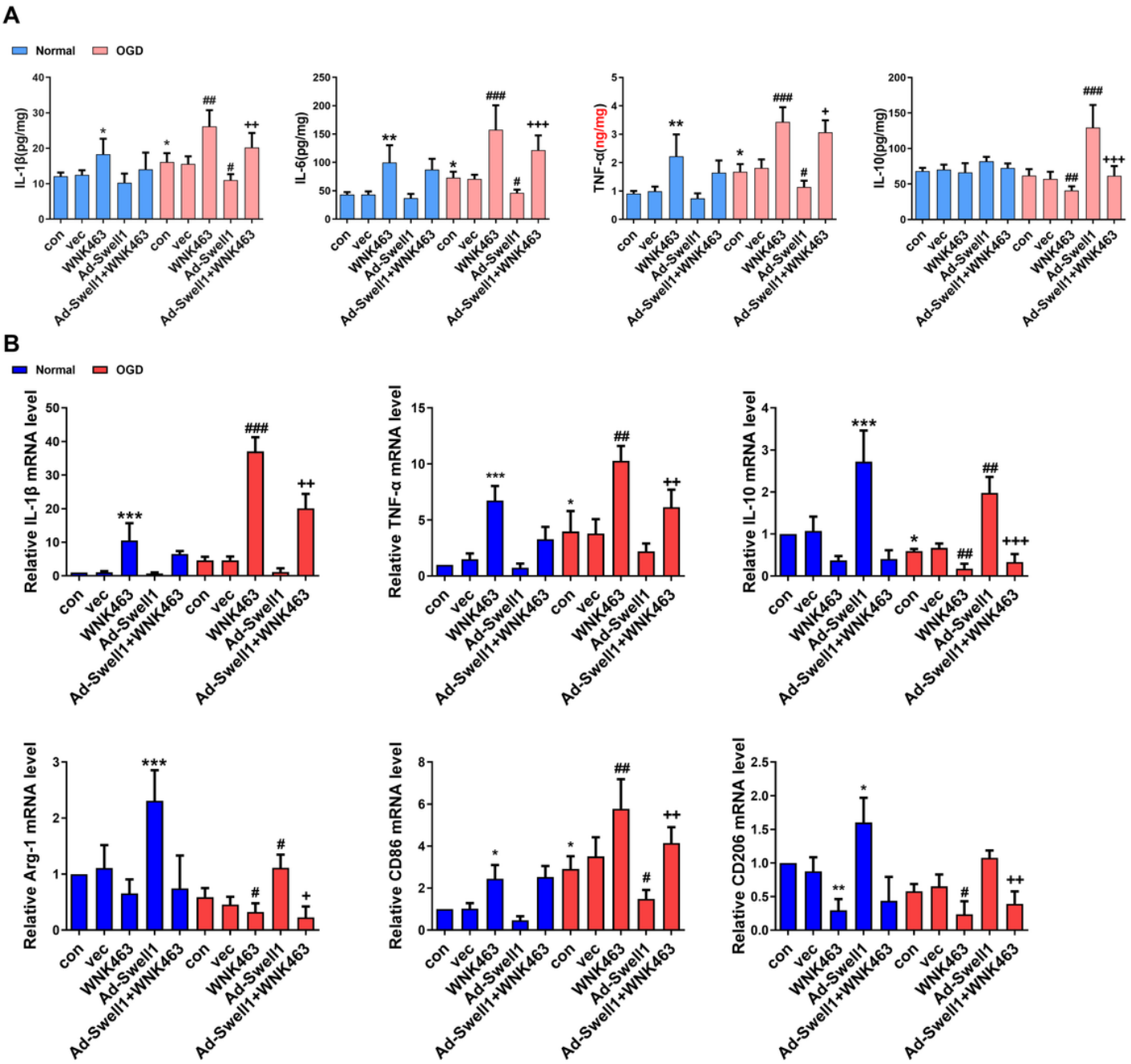

Figure 8

Inhibition of WNK kinases blocks microglia M2-polarization promoted by Swell1 channel after OGD.

A and B, BV2 cells were transfected with Swell1 expressed adenovirus for 24 h, or (and) just pretreated with WNK463 (100mM) for 6 h before OGD treatment as indicated. The effect of Swell1 and WNK463 on the inflammation-related factors IL-1β, IL-6, IL-10 and TNF-α expression was measured by Elisa (A), while IL-1β, IL-10, Arg-1, TNF-α, CD86 and CD206 at mRNA levels was detected by RT-PCR (B). n=5, Tukey's multiple comparisons test, *p<0.05 *vs.* con-Normal, $^{\#}$p<0.05 *vs.* con-OGD, $^{+}$p<0.05 *vs.* Ad-Swell1-OGD, ** p<0.01 *vs.* con-Normal, $^{\#\#}$ p<0.01 *vs.* con-OGD, $^{++}$ p<0.01 *vs.* Ad-Swell1-OGD, *** p<0.001 *vs.* con-Normal, $^{\#\#\#}$ p<0.001 *vs.* con-OGD, $^{+++}$ p<0.001 *vs.* Ad-Swell1-OGD.

Supplementary Files

This is a list of supplementary files associated with this preprint. Click to download.

- Supplementarymaterials.docx